Numerical Predictions of the Load-Displacement Curves of Rock-Socketed Concrete Piles

Kwon, Oh-Sung*1 Kim, Jeong-Hwan*2
Jeon, Kyung-Soo*3 Kim, Myoung-Mo*4

요 지

암반 근입말뚝의 설계기준은 일반적으로 침하량 기준을 사용하므로 설계단계에서 암반근입말뚝의 하중-변위(σ-δ) 거동을 잘 이해해야 하나 그 거동의 복잡성으로 인해 하중-변위 거동을 파악하기가 어렵다.

이를 위해 먼저 현장타설 콘크리트 말뚝에 대해 현장재하시험을 실시하여 그 결과로부터 암반근입말뚝의 하중-변위 거동을 고찰하였고, 상용 프로그램인 FLAC을 이용하여 하중-변위 곡선의 형상에 큰 영향을 주는 입력변수를 변화시켜 가며 말뚝의 하중-변위 관계를 모사하였다. 최종적으로 수치해석 입력데이터와 현장 지반조사결과의 관계를 일반화함으로써 지반공학자가 설계단계에서 적절한 현장데이터를 이용하여 하중-변위 거동을 예측할 수 있도록 하였다.

Abstract

The settlement limit concept is generally adopted as design criteria of rock-socketed pile foundations, therefore, the load-displacement(σ-δ) behavior of the rock-socketed piles should be well understood at the design stage, which, however, is hard to achieve due to its complexity. To help this out, field pile load tests are executed on cast-in-situ concrete piles, first, to figure out the σ-δ behavior of rock-socketed piles. Next, the σ-δ relations of the piles are simulated numerically using commercial package program(FLAC) varying a couple of input data which are sensitive in shaping the σ-δ curves. Finally, the relation between the best input data for the numerical simulations and the geotechnical field data are cultivated to generalize the numerical simulation procedures, which enables geotechnical engineers to predict the σ-δ behavior at the design stage, if appropriate geotechnical field data are provided.

Keywords: Rock-socketed pile, Load-displacement curve, Pile load test, Interface element, Peak cohesion, Subgrade reaction modulus

*1 Member, Department of Civil Eng., Seoul National University
*2 Member, Institute of Technology, Engineering & Constitution Group, Samsung Corporation
*3 Member, Geotechnical Research Division, Korea Highway Corporation.
*4 Member, Professor, Department of Civil Eng., Seoul National University

1. Introduction

It is known that the allowable bearing capacity of rock-socketed piles is governed exclusively by the settlement, and not by strength, unless the strength of the intact rock is extremely low. Thus, to be able to predict the capacity of the rock-socketed piles, the load displacement(σ-δ) behavior of the piles should be well understood.

To this end, a series of field load tests are executed on cast-in-situ concrete piles to obtain the σ-δ curves, which are, then, simulated by numerical manipulation. In the manipulation, input data of a couple of geotechnical constants are varied to find out the best values to simulate the field curves. After obtaining a set of the best input data, the relationships between the input data and geotechnical properties of base rocks are cultivated so that the field σ-δ curves could be numerically predicted, if the field geotechnical properties are given.

2. Pile Load Tests

The base rock of the test site is Gneiss which is one of the most popular types of rocks in Korea. 8 of 40cm cast-in-situ piles are constructed on the site with 2 anchor piles for each test pile(Kim, 1997). Plan view of the test pile arrangement as well as the location of boreholes is shown in Fig.1, and the boring logs, in Fig.2. NX boring is executed to estimate rock mass property after pile load tests. The results are illustrated in Fig.3, together with pressuremeter and uniaxial compression tests results.

Pile No.1 is intended to penetrate the base rock by one pile diameter, and, to eliminate the point resistance, styrofoams of 10cm thickness are stacked at the bottom. Rock penetration depthes of Piles No.2~No.7 vary from 0.5~2.7 times of the pile diameter as listed in Table 2(Pile No.3 is eliminated in the table because it is constructed for different purpose). Pile No.8 is constructed through soil layers only, and styrofoam of 10cm thickness are stacked at the bottom.

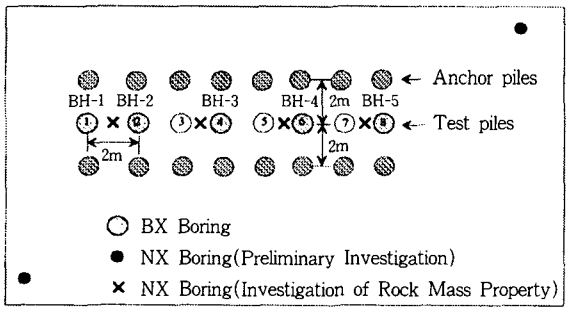

Fig. 1 Plan view of test piles

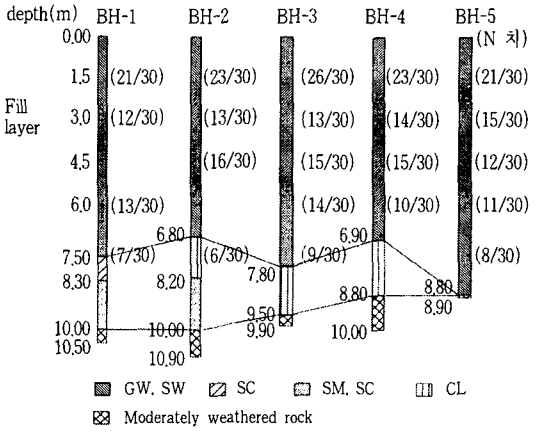

Fig. 2 Soil profile

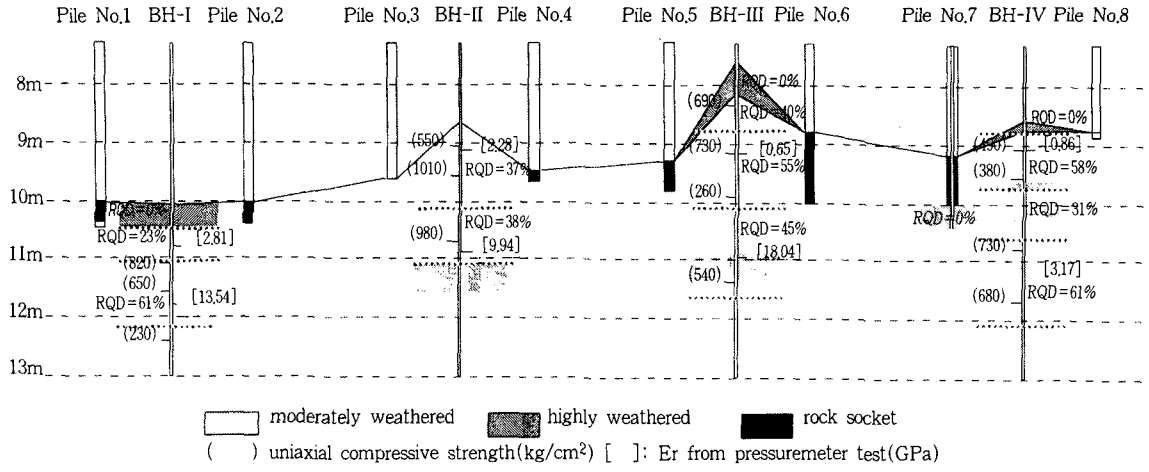

Fig. 3 Results of NX boring, pressurmeter test, and uniaxial compression tests

Pile load tests are executed following ASTMD 1143-81. The whole test results are shown in Fig.4.

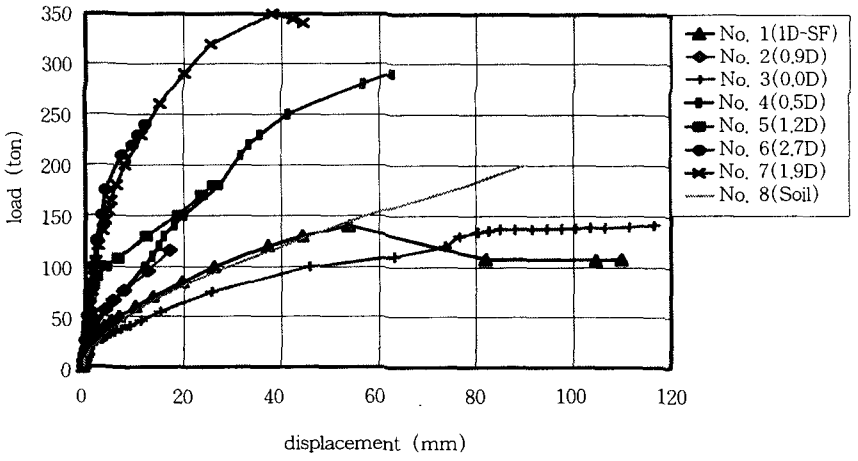

Fig. 4 Pile load test results

3. Numerical Manipulation

Flac

Package program FLAC has been utilized to reproduce the field vertical load-displacement curves by numerical manipulation. In the manipulation, elastic piles are modeled axisymmetrically, and surrounding soils are simulated by elasto-plastic constitutive models obeying Mohr-Coulomb's failure criteria. The finite difference grid used in the numerical simulation is shown in Fig.5.

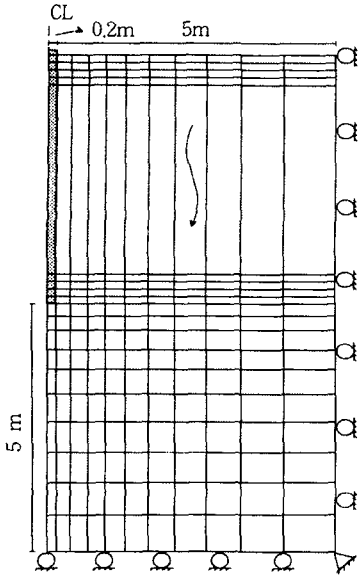

Fig. 5 Finite difference grid

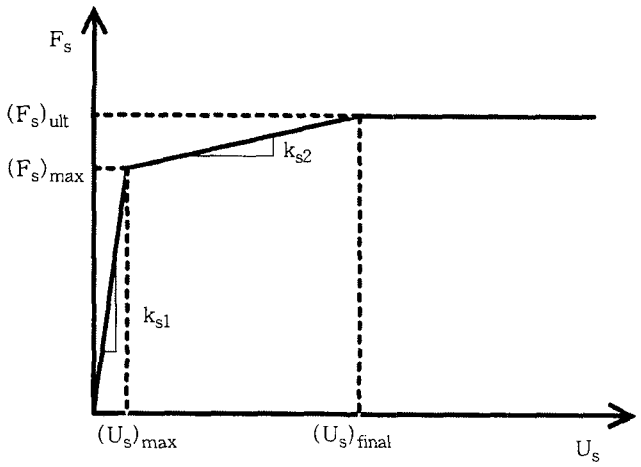

Fig. 6 Shear force versus displacement

Interface Elements

To simulate the slip of piles along the pile-soil boundaries, interface spring elements are employed at the boundaries(Cundall, 1976). For normal action at the boundaries, the contact force, F_n, is evaluated in terms of the normal stiffness, k_n, of the contact, and the notional displacement, u_n, from the expression

$$F_n = k_n u_n \tag{1}$$

For shear force, F_s exerted at the interface due to the shear displacement, u_s between the pile and the soil, it is evaluated from the similar expression using the shear stiffness, k_s

$$F_s = k_s u_s \tag{2}$$

Both stiffnesses of interface shown above are assumed to have dual values depending upon whether slip along the pile-soil boundary has occurred. Before the slip occurring, k_{s1} is calculated assuming $(u_s)_{max}$ (Fig.6) to be as small as 0.1mm, which will make the resulting load-displacement curve to follow the elastic compression line of a pile. Meanwhile, k_{s2}, after the slip, is calculated using $(u_s)_{final}$ (Fig.6) of several millimeters, and the residual shear resistance coming from dilation of the slip surface, ΔF_s is evaluated from the expression(Cundall, 1976),

$$\Delta F_s = F_s - (F_s)_{max} = k_{s2}\Delta u_s = k_{s2}(u_s - (u_s)_{max}) \tag{3}$$

And $(F_s)_{ultimate}$ in Fig.6 can be expressed as(Patton, 1966)

$$(F_s)_{ult} = A \cdot (c_{residual} + \bar{\sigma}_n \tan(\phi + \varphi)) \quad (4)$$

, where A: contact area, $\bar{\sigma}_n \tan$: effective normal stress, $c_{residual}$: pile-soil adhesion, ϕ : pile-soil friction angle, φ: dilation angle.

The values of u_s may be compared with the model test results of Pells et.al(1980), in which $(u_s)_{max}$ ranged from 0.5 to 3mm, and $(u_s)_{final}$, 10mm. For the k_n before the slip, horizontal subsurface reaction modulus, k_h, obtained from pressuremeter test(PMT) is used, and after the slip, it is assumed to be 10 times of the value of k_s as suggested by Belytschco et. al(1984).

4. Numerical Simulation of Field Load Test Curves

To take care of the effect of soil layers around the pile shaft on the load-displacement behavior, the load-displacement curve of pile No.8 which is embedded only in the soil layers with styrofoam stacked at the bottom is simulated first. As seen in Fig.7, the fore part of the curve can be simulated reasonably well by the numerical manipulation under the assumption of no point resistance. However, since rear part of the curve is affected by the point resistance exerted from the styrofoam bottom after it is deformed to a critical state, it shows a big discrepancy between the field curve and the numerically predicted one. To quantify the stress-strain behavior of styrofoam, a triaxial test is executed on a styrofoam specimen(E = 120kPa), whose result is shown in Fig.8. Referring to this figure, point resistance is assumed to occur from the base rock after the styrofoam is squeezed more than 90% of its length, which is taken into account in numerical prediction by replacing styrofoam element properties with those of rock as shown in Fig.7 by a dashed line. The resulting σ-δ curve after 40mm settlement shows similar trend to that of the field load test.

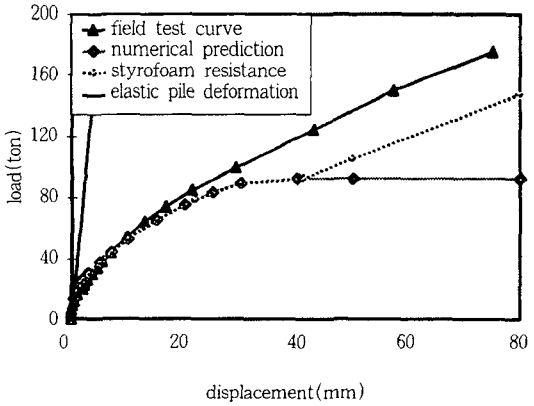

Fig. 7 Pile No.8

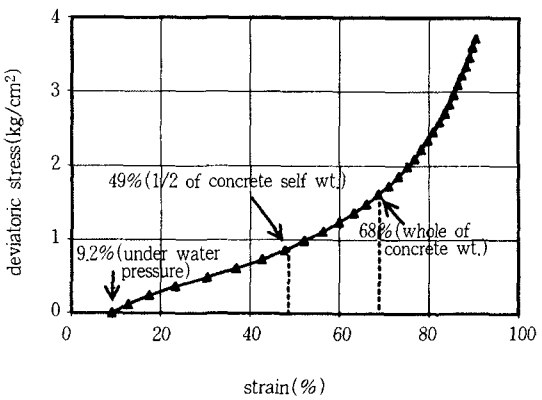

Fig. 8 Triaxial test result on styrofoam

Geotechnical property data of soil layers used in the simulation of rock-socketed piles are listed in Table 1. The angles of internal friction are obtained empirically from N values of SPT, and the dilation angles are adjusted to produce similar σ-δ curves to the field ones. For the part of piles embedded through soil layers, the dilation angle is found to play a decisive role in determining the shape of σ-δ curves because adhesive resistance between the pile and soil is negligible in most cases.

Table. 1 Geotechnical property

Geo-data / Unified classification of soils	E (MPa)	ν	γ_t (t/m^3)	ϕ (°)	ψ (°)
GW, SW(Fill)	40	0.3	1.9	34	20
SC, SM	20	0.3	1.8	32	5
CL	10	0.3	1.8	28	0

Generally, it is known that the very first part of the σ-δ curve of rock-socketed piles is affected by the lateral deformation modulus of the wall rock, and the elastic limit, by the magnitude of the adhesion between pile and rock mass. The σ-δ behavior after slip is mostly affected by the vertical subgrade reaction modulus of the pile base following the reduction of pile-rock adhesion due to the superposition of the pile and adjacent soils(Carter & Kulhawy(1988), Kulhawy & Goodman(1987)). Therefore, the peak cohesion before slip, c_{peak}, and the vertical reaction modulus of the base, k_b, are varied to produce similar σ-δ curves to those of field tests. After slip, the residual value of pile-rock adhesion($c_{residual}$) is assumed to be 1/2 of c_{peak}. Fig.9 shows one of the resulting σ-δ curve obtained numerically, which matches very well with the field curve. In the same figure, the σ-δ curve of the rock-socketed portion of a pile is also shown which is obtained by eliminating shaft resistance of soil layers from the total σ-δ curve. The σ-δ curve of rock-socketed

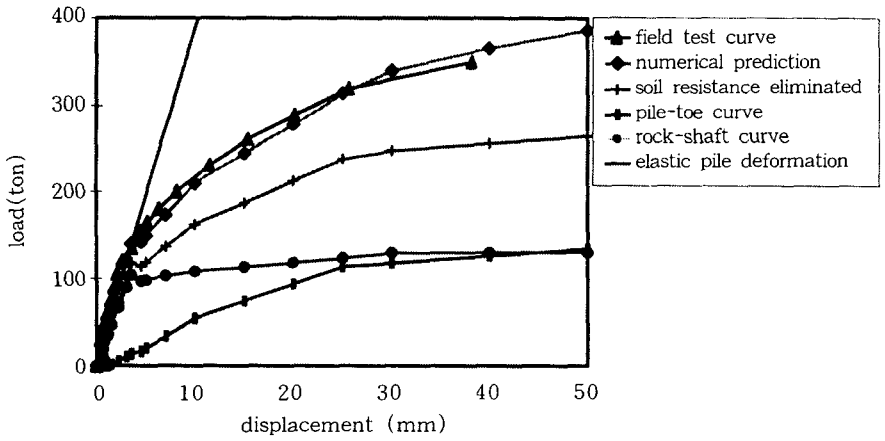

Fig. 9 Pile No.7

portion of the pile is, then, separated into the σ-δ curve of the shaft and the point of the pile as shown in the same figure. The σ-δ curve of the shaft shows the elastic-perfectly plastic behavior, and that of the point increases monotonically to a great extent of the pile settlement, which agrees with the observation of Carter and Kulhawy(1988).

In Table 2, the input data used to simulate the σ-δ curves of rock-socketed part of piles are tabulated with the geotechnical properties of the base rock masses. As stated in the table, the internal friction angle and the dilation angle are fixed at 40° and 10°, respectively, which is justified because the variation of those angles has very limited influence on the result.

Table.2 Geotechnical properties and manipulation data of the rock masses

Result of experimental and numerical manipulation \ Pile No.(Embedment depth)		1 (1.0D)	2 (0.9D)	4 (0.5D)	5 (1.2D)	6 (2.7D0	7 (1.9D)
Field & laboratory test data	Lateral deformation modulus of rock mass from PMT(GPa)	2.81	2.81	6.11	9.35	9.35	–
	Unconfined compressive strength of intact rock, q_u (MPa)	23.0	23.0	78.0	49.5	49.5	43.5
	RQD	12	12	37	47	47	45
	Rock Mass Rating(RM)	28	28	35	40	40	40
Input data for simulation	Pile-soil adhesion, c(kPa)	150	600	800	1200	1200	1200
	Reaction modulus(kPa/inch)	–	1400	3000	1000	4000	6000
	Friction angle, ϕ (°)	40°					
	Dilation angle, ψ (°)	10°					

5. Predicted σ-δ Curves

To generalize the numerical simulation procedure, it is necessary to find out the relations of the input data used in the simulation with the geotechnical field data such as the deformation modulus from PMT, the unconfined compressive strength of rocks(q_u), RQD, and the Rock Mass Rating(RMR) of Bieniawski(1976). They are plotted in Figs. 10~13 for c_{peak}, and in Figs.14~17 for k_b. All show good relations except the q_u. The equations of the respective regression lines are shown in Eqs.5~7, disregarding pile No.1, for c_{peak}, and Eqs.8~10, disregarding pile No.5, for k_b. Repredicted σ-δ curves are shown in Figs.18~22, for which Eq.5 is used for c_{peak}, and Eq.8 for k_b except for the pile No.7. Eq.10 is used for k_b of the pile No.7 due to the lack of the deformation modulus data from PMT for that particular pile. From the comparisons of the field curves with the predicted ones in the figures, and from the inspection of the correlation coefficients of the regression lines in Figs.10~12 and Figs.14~16, it is concluded that any of the equations can be

used to simulate the σ-δ curves of rock socketed piles in compliance with the availability of geotechnical field data.

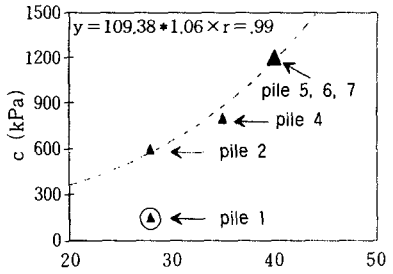

Fig. 10 c_{peak} vs. RMR

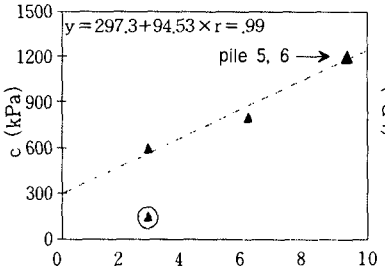

Fig. 11 c_{peak} vs. E_r

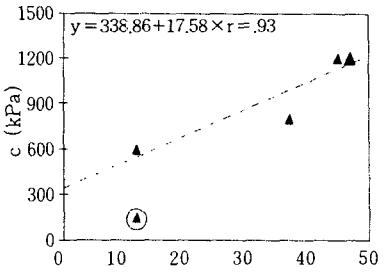

Fig. 12 c_{peak} vs. RQD

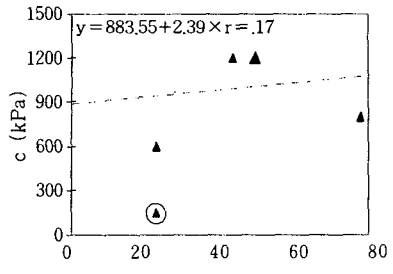

Fig. 13 c_{peak} vs. q_u

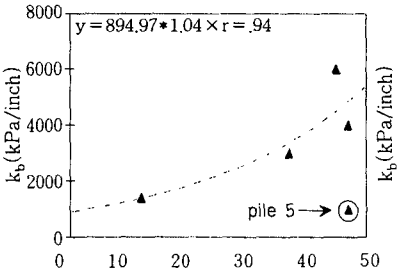

Fig. 14 k_b vs. RQD

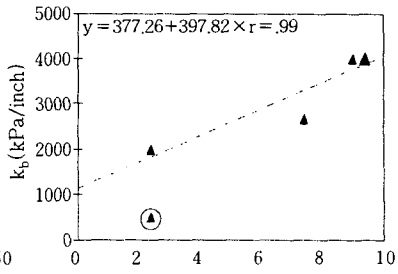

Fig. 15 k_b vs. E_r

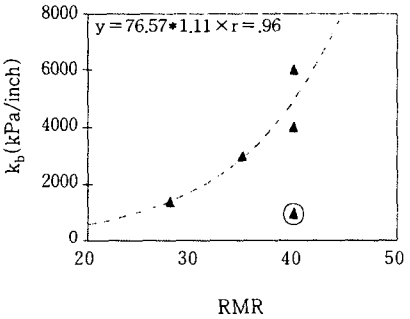

Fig. 16 k_b vs. RMR

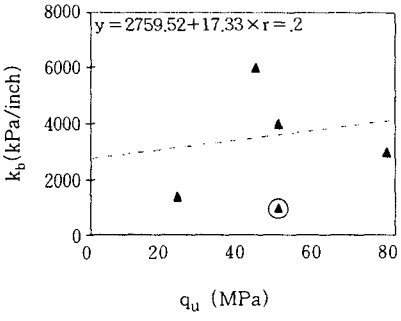

Fig. 17 k_b vs. q_u

$$c(kPa) = 109 \times 1.06^{RMR} \quad (5)$$

$$c(kPa) = 297 + 95 \times E_r(GPa) \quad (6)$$

$$c(kPa) = 339 + 18 \times RQD(\%) \quad (7)$$

$$k_b(kPa/inch) = 378 + 398 \times E_r(GPa) \quad (8)$$

$$k_b(kPa/inch) = 895 \times 1.04^{RQD} \quad (9)$$

$$k_b(kPa/inch) = 77 \times 1.11^{RMR} \quad (10)$$

where E_r = deformation modulus from PMT, k_b = vertical subgrade reaction modulus of the base.

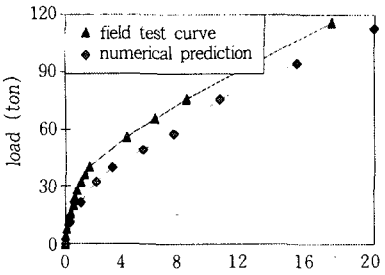

Fig. 18 Pile No.2

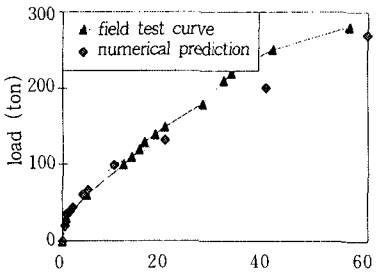

Fig. 19 Pile No.4

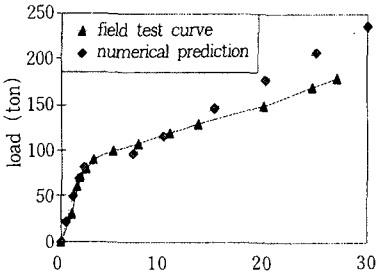

Fig. 20 Pile No.5

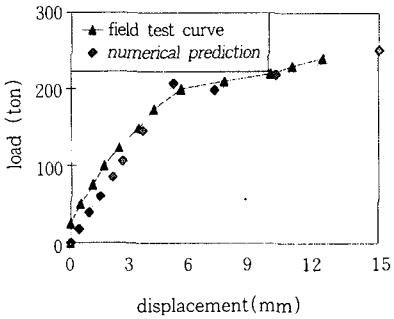

Fig. 21 Pile No.6

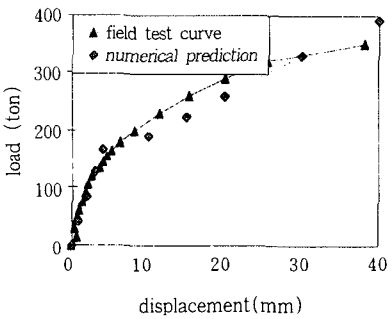

Fig. 22 Pile No.7

6. Conclusions

From a series of field pile load tests on the rock-socketed cast-in-situ concrete piles of 40cm diameter, and numerical simulation works, the followings are drawn as conclusions.

1) In simulating the load-displacement behavior of rock-socketed piles numerically, the rolls of the peak cohesion intercept, c_{peak}, and the vertical subgrade reaction modulus of the base rock, k_b, are found to be very important, which can be estimated reasonably well from geotechnical field data, such as the deformation modulus from PMT, RQD, or RMR values, using the empirical expressions as suggested in this paper.
2) Since the empirical expressions suggested here are verified only for the cases from which the empirical relations are extracted, further verification processes are needed.

References

1. Belytschko, T., Plesha, M., and Dowding, C. H., A computer method for stability analysis of caverns in jointed rock, International Journal for numerical method in geomechanics, Vol. 8, 1984, pp. 473~492.
2. Bieniwski, Z. T., Rock mass classifications in rock engineering, Proc. Symp. exploration for Rock Engineering, Bieniwski, Z. T.(ed.), Vol.1, A. A. Balkema, Rotterdam, 1976, pp. 97~106.
3. Carter, J. P. and Kulhawy, F. H., Analysis and design of drilled shaft foundations socketed into rock, Report EL-5918, Electric power research institute, Palo Alto, California, 1988, pp. 188.
4. Cundall, P. A., Explicit finite difference methods in geomechanics, In numerical methods in engineering, proceedings of the EF conference on numerical methods in geomechanics, Blacsburg, VA, Desai, C. S.(ed.) Vol. 1, 1976, pp. 132~150.
5. Kim, J. H., Analysis of resistant behaviour of cast in-situ concrete piles socketed in gneiss, PhD thesis, Seoul National University, Seoul, Korea, 1997.
6. Kulhawy, F. H. and Goodman, R. E., Foundations in Rock, Chapter 55 in Ground engineers reference book, Bell, F. G.(ed.), Butterworths, London, 1987.
7. Patton, F. D., Multiple modes of shear failure in rock and related materials, PhD thesis, University of Illinois, Urbana, 1966.
8. Pells, P. J. N., and Rowe, R. K., and Turner, R. M., An experimental investigation into side shear for socketed piles in sandstone, In proceedings, Conference on structural foundations on rock, Pells, P. J. N.(ed.), Sydney, Australia, Vol. 1, 1980, pp. 291~302.

(received on Apr., 21. 1999)